



Measurement and modelling of near-tip displacement fields for fatigue cracks in 6082 T6 aluminium

D. Nowell, M.E. Kartal

Department of Engineering Science, University of Oxford, Oxford, (UK)
david.nowell@eng.ox.ac.uk

P.F.P de Matos

U3Is, Unidade de Investigação e Internacionalização, ISVOUGA, Santa Maria da Feira, (Portugal)

ABSTRACT. Recent work by de Matos and co-workers has used digital image correlation to examine the surface displacements in the near-tip region of a propagating fatigue crack. The primary purpose of the experiments was to investigate crack closure, and successful measurements were made. However, the data collected can also be used to investigate the more general in-plane displacement field in the neighbourhood of the crack tip and to compare this with alternative models for near-tip displacements. Experiments were undertaken using CCT specimens manufactured from 6082 T6 aluminium alloy. Three different specimen thicknesses were examined (3, 10, and 25mm), in order to examine the effect of this parameter on the measured displacements, closure levels, and crack propagation rates. The current paper re-analyses the experimental measurements by evaluating crack face displacements as a function of loading for a region close (i.e. within 500 μm) to the crack tip. These provide an excellent means of validating proposed models of crack tip stresses, strains, and displacements. The measurements will be compared to the predictions of classical crack tip models (such as the Westergaard solution, together with a recent elastic-plastic model, proposed by Pommier and co-workers, which partitions the field into elastic and plastic components. The results of these comparisons are discussed and recommendations made for future experimental work.

KEYWORDS. Digital image correlation; displacement measurement; crack-tip fields.

INTRODUCTION

The characterisation of crack tip stress fields has been a subject of study since the very beginnings of fracture mechanics, and an excellent collection of classical papers can be found in the two-volume compilation edited by Sanford [1], [1]. Inglis' paper of 1913 [2] recognises that, in an elastic material, the stress will be singular at a sharp crack tip. Twenty five years later, Westergaard produced the stress solution for a crack in an elastic medium which forms the basis of the stress intensity factor concept. However, it was not until 1957 that Irwin [4] formalised the definition of the stress intensity factor and connected the stress-based approach to the earlier energy-based analysis of Griffith [5]. Building on these foundations, the concept of the stress intensity factor as a similitude parameter for characterising the fracture behaviour of cracks has become widely established. The concept was extended from uniaxial loading to the analysis of fatigue cracks by Paris and co-workers, leading to the formulation of the 'Paris Law' in 1963 [6]. K and ΔK have proved to be extremely useful parameters, but it has been widely recognised that there are limitations to their



applicability. The usefulness of K in characterising the crack tip stress field relies on the concept of small-scale yielding, so that the leading term in the series expansion for the stresses at the crack tip can be taken to characterise the strains within the crack tip process zone. In practice, the K -based approach is found to be useful, even when small-scale yielding is not as well satisfied as we would like. Nevertheless, there remain many situations where the plastic zone is larger than the K -dominated region around the crack tip. Recognition of this feature has led to the development of elastic-plastic fracture mechanics, including the use of the J -integral parameter [7] to characterise conditions at the tip of a crack tip with a significant plastic zone.

The foundations of fracture mechanics were built using the tools of analytical stress analysis. Over the past 40 years, these have been supplemented by powerful numerical stress analysis techniques, particularly the finite element method [8]. These have allowed the analysis of crack tip stress fields to a level of detail previously unattainable and have allowed detailed investigation of phenomena such as plasticity-induced fatigue crack closure [9] and complex corner singularities [10]. It has also been possible to capture more realistic material behaviour. Nevertheless, such simulations have their limitations. For example, finite element methods treat the material as a continuum, and ideal isotropic material behaviour is often assumed. However, in practice the area of high stress surrounding a crack tip is often comparable with the grain size of the material. This means that the assumptions of continuum elasticity and plasticity can sometimes be called into question. Hence, there is a long history of experimental work in the field of fracture mechanics, attempting to characterise the crack tip stress fields in real cracks and comparing them to the analytical and numerical solutions discussed above.

It is not appropriate here to provide a comprehensive review of the techniques used to investigate crack tip stress fields experimentally. Nevertheless, a brief overview of early work provides a useful background to our current work. A wide range of techniques have been employed, including photoelasticity [11]; caustics [12]; and interferometric approaches such as moiré [13]. These have become useful tools, but they are still experimentally demanding and have a number of disadvantages, including that the range of materials to be investigated can be limited (e.g. in the case of transmission photoelasticity). Recent advances in image processing techniques, together with the widespread availability of low-cost digital cameras, have led to a dramatic rise in the use of digital image correlation for the analysis of cracks, either for the measurement of fatigue crack closure [14], [15] or for the determination of stress intensity factors [16]. By its nature, digital image correlation involves the analysis of surface deformations, but recent work using X-Ray Synchrotron experiments and volume correlation has extended this to full three-dimensional measurement of crack tip stress fields [17].

Hence, there has been a renewed interest in the characterisation of crack tip stress fields, with the objective of building on the understanding of classical fracture mechanics. In particular, there is a desire to understand phenomena which are currently difficult to predict, such as the effect of load (R -) ratio or non-uniform loading on growth rates of a fatigue crack. The availability of sophisticated tools for numerical stress analysis, combined with relatively straightforward measurement techniques such as DIC has provided a significant stimulus for work in this area. The aim of the current paper is to examine in more detail some measurements reported by de Matos and Nowell [18], [19], made in the context of an investigation of fatigue crack closure. These will be re-analysed in order to examine the implications of the measurements for crack tip stress, strain and displacement fields. In particular, results for the opening displacement of cracks will be obtained as a function of load and these will be compared to the predictions of a recent two-parameter model of crack tip stress suggested by Pommier and co-workers [20].

EXPERIMENTAL WORK

The fatigue experiments carried out by de Matos have been described elsewhere [18],[19] and are described in greater detail in [21]. Hence, only a brief overview will be given here, so that the reader can understand the context of the experimental measurements. CT specimens were manufactured from 6082 T6 aluminium alloy in three different thicknesses (3, 10, and 25 mm). The (engineering) yield stress of the material was measured by means of a simple uniaxial experiment and was found to be 323 ± 5 MPa. The material exhibited relatively little work-hardening, and the UTS was around 330 MPa at a nominal strain of 0.07. The specimens were initially pre-cracked and then tested in a servo-hydraulic fatigue machine. Instrumentation was provided in a number of different forms: a conventional load cell measured load on the specimen, and a strain gauge was provided on the back face of the specimen (opposite the crack tip). A conventional 'Elber gauge' was used to measure crack opening displacement and, together with the back face strain gauge, this enabled the use of compliance methods to estimate crack opening loads. Crack length was measured optically, using a video camera on one side of the specimen. On the other side of the specimen, a 'Questar' long range

microscope [22] was mounted on a translation stage. This could be used to measure crack length, but also to acquire images of the area close to the crack tip using a low-cost commercial USB webcam. Fig. 1 shows an overview of the specimen geometry and of the experimental configuration. The microscope was focussed so as to give a field of view of 0.6×0.45 mm near to the crack tip and this was recorded at a resolution of 640×480 , giving a pixel size of $0.93 \mu\text{m}$. Loading was carried out at a range of loads ($1.5\text{kN} > P_{\text{max}} > 12.5 \text{ kN}$) and with $R = 0.1$ or 0.125 . Images were collected at 30 fps whilst cycling the specimen at a reduced rate of 0.25Hz . This gave 360 frames per measurement, recorded over 3 cycles of loading. Measurements were repeated at a number of different crack lengths during propagation of the crack.

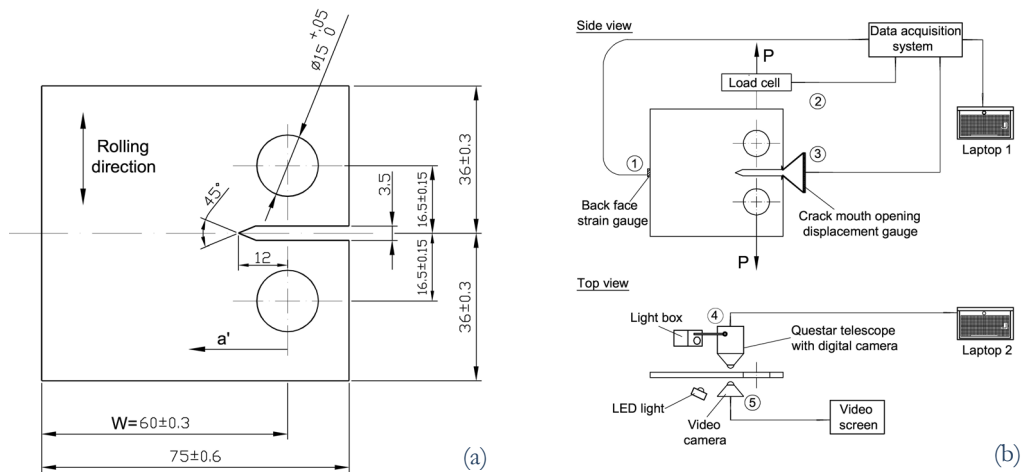


Figure 1: (a) Specimen geometry (side view); (b) experimental configuration.

Fig. 2 (a) shows a typical recorded image. It will be noted that most of the field of view is located behind, rather than in front of, the crack tip. This is because the primary purpose of the original experiments was to investigate crack closure and direct measurements of the crack wake were preferred. Once the images had been acquired, displacements were calculated using digital image correlation using the public domain software written by Eberl et al [23]. The amount of data collected was quite significant and it was therefore decided not to analyse the complete displacement field for each image. Instead, five pairs of locations, separated by $100 \mu\text{m}$ along the crack direction were chosen for analysis (see Fig. 2).

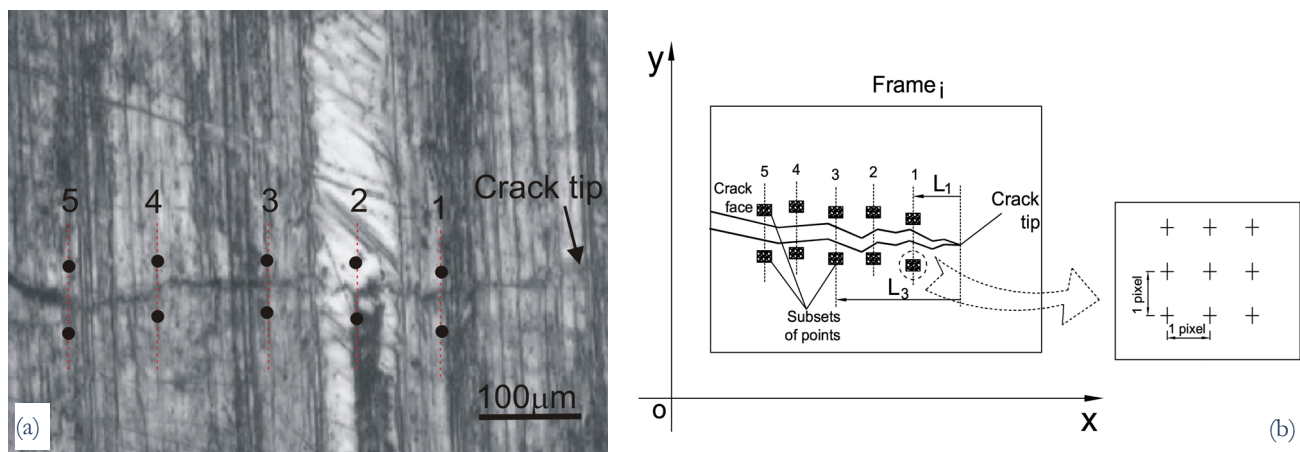


Figure 2: (a) Typical recorded image, showing locations at which displacement was calculated; (b) schematic diagram showing use of 9 points at each location to give better quality results.

At each location, 9 points in a 2×2 pixel array were selected for analysis (see Fig. 2b) and the results of these calculations were averaged at each location to reduce scatter in the results. The displacements obtained at each pair of locations were



then compared to obtain a value for relative displacement at each of the pairs of locations (1-5, Fig. 2). As expected, the relative displacement varied with load and was approximately sinusoidal with time, corresponding to the cyclic load applied (Fig. 3a). However, it is apparent in Fig. 3(a) that there is a period at low load when the relative displacement does not change. This can be interpreted as the time during which the crack is closed at the location of the measurement. Relative displacement can also be plotted directly against load (Fig. 3b), and it can be seen that there is clear evidence of crack closure. At each measurement location, there is very little variation of relative displacement with load until a critical value of load is reached, P_{open} , when the crack opens and a nearly linear variation is exhibited. Points further away from the crack tip (e.g. L_5) open at lower loads than those near the tip (e.g. L_1), indicating that the crack peels open from the mouth to the tip.

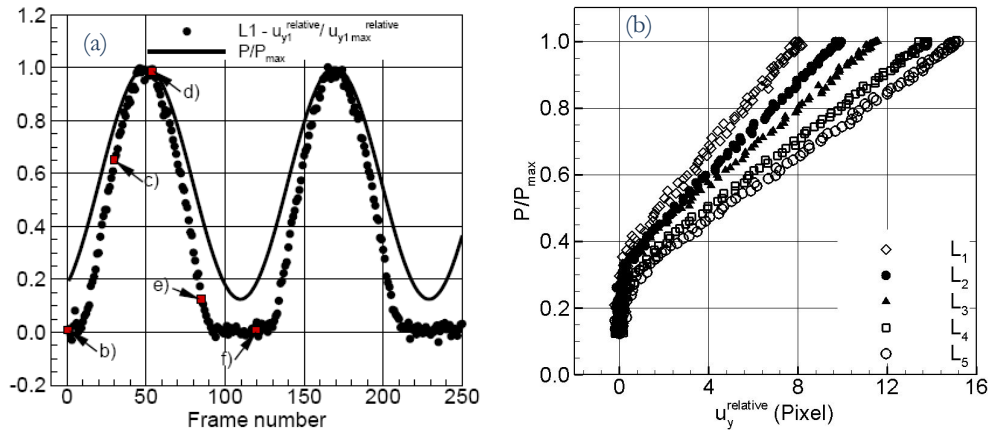


Figure 3: (a) Typical variation of relative displacement (u_{y1}) with time (frame number) compared to the sinusoidal applied load (P); (b) Relative displacement plotted against load, for 5 different measurement locations L_1 to L_5 (Fig. 2).

RESULTS AND ANALYSIS

Although the original experiments were carried out to measure crack closure, the primary focus of the current paper is not in this area, other than that any closure present will affect the crack tip stress fields. As was highlighted earlier, the amount of information recorded ahead of the crack tip is quite limited. However, measurements of crack opening, u_y , at different locations along the crack may usefully be used to assess the accuracy of different models of crack tip deformation and to experimentally obtain parameters which characterise crack loading. According to the conventional elastic model for a sharp crack, the displacement along the crack faces is given by

$$u_i(r) = \pm \frac{4K_I}{E} \sqrt{\frac{r}{2\pi}} \quad (1)$$

in plane stress, where K_I is the mode I stress intensity factor, E is Young's Modulus (taken as 70GPa for the alloy under investigation), and r is the distance from the crack tip. In (1), the positive sign corresponds to the upper crack face and the negative sign to the lower one, so that the relative displacement between points on the two faces is given by

$$u_y(r) = \frac{8K_I}{E} \sqrt{\frac{r}{2\pi}} \quad (2)$$

Hence, a plot of $\log(u_y)$ against $\log(r)$ should give a straight line with a gradient of 0.5. Fig. 4(a) shows a typical set of results obtained from a 25 mm thick specimen at a mean crack length of 11.7 mm with a maximum load of 12.5 kN and an R ratio of 1.0. In this figure, four different loads are shown, corresponding to P/P_{max} between 0.504 and 1.0 (during the loading part of the cycle). At lower loads than this, the crack is closed over much of the field of view. It can be seen that the log/log plot does give an approximately linear relationship between u_y and r as implied by (2), and at maximum

load we obtain $u_r \propto r^{0.508}$ with a correlation coefficient of 0.99. Note that, in producing this plot, we have taken the distance between the first set of measurement points and the crack tip to equal the nominal value of 100 μm . However, in common with many image correlation techniques applied to crack problems, it is not possible to know where the crack tip is with absolute precision and, in any case, the position of the crack front may vary through the thickness of the specimen so that a surface value may not be wholly representative. It is therefore advisable to undertake a fitting procedure to determine the crack tip position by reference to the data. However, in the current example, it is found that introducing an offset of greater than about 10 pixels (9.3 μm) significantly worsens the quality of the data fit. It should be noted, however, that in Fig. 4(a) the slope of the lower line is significantly different from those obtained at the higher loads ($u_r \propto r^{0.67}$ with a correlation coefficient of 0.96). This suggests that (1) and (2) do not provide such a good fit to the experimental data when the crack has only just opened.

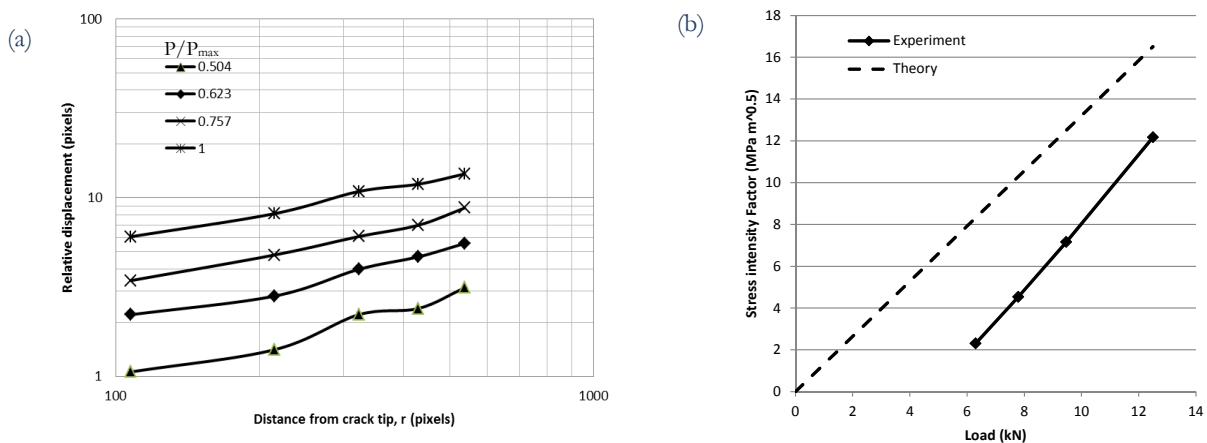


Figure 4: (a) Typical variation of relative displacement (u_{y1}) with distance from the crack tip (r) at four different values of load (P/P_{\max}); (b) Stress intensity factors measured from displacement data and calculated from the load and the theoretical SIF expression for the specimen geometry.

The data plotted in Fig. 4(a) can be used to obtain a value for the stress intensity factor using equation (2). This may be compared to the nominal value of K for the geometry of specimen used and load applied [25]. Data fitting is carried out for each load using the five available points and a least squares procedure. The results of this calculation are displayed in Fig. 4b. It can be seen that the experimental results show an excellent linear relationship between load and K ($R^2 = 0.9995$), and that the slope of the line is very similar to that predicted by the theoretical SIF based on average crack length. However, there is an offset to the experimental line, suggesting that K is zero for a load of 4.9 kN (39% of the maximum applied load). An alternative way of explaining this behaviour is the existence of a residual K of $-7.8 \text{ MPa m}^{0.5}$ caused by crack closure and the associated residual compressive stresses which exist between the crack faces at zero load¹.

Elastic-plastic model

Pommier and co-workers have developed a finite element approach [20] to the prediction of fatigue crack behaviour which relies on the decomposition of the crack tip stress field into elastic and plastic components. If we concentrate on mode I loading, the displacement will be expressed as

$$u = K_I u_{el} + \rho u_{pl} \quad (3)$$

where K_I is the standard mode I stress intensity factor and ρ is an equivalent scaling factor for the plastic field (effectively equal to the crack tip opening displacement). The quantities u_{el} and u_{pl} are respectively the elastic and plastic components of the stress field caused by a unit K or ρ . u_{el} is simply that implied by the Westergaard solution [3], whereas u_{pl} can be obtained (to a first approximation) by the displacement field resulting from a unit dislocation at the crack tip, with the

¹ It should be realised, of course, that a negative stress intensity factor has no physical meaning on its own, but it is a convenient concept in a superposition argument when combined the applied value, provided that the total $K > 0$.



branch cut along the crack (i.e. a constant displacement along the crack). Once these parameters have been defined, it is possible to investigate the behaviour of the crack K / ρ space. Model predictions suggest that some phases of loading (e.g. initial loading from zero, or initial unloading) result in largely elastic behaviour (i.e. a change in K , but not in ρ) and this can be interpreted as a reason for the existence of a threshold ΔK since crack extension is only likely to occur if there is a change in the plastic part of the displacement field (i.e. ρ) during a given increment of load. Figure 5(a) shows a schematic of crack behaviour in crack K / ρ space.

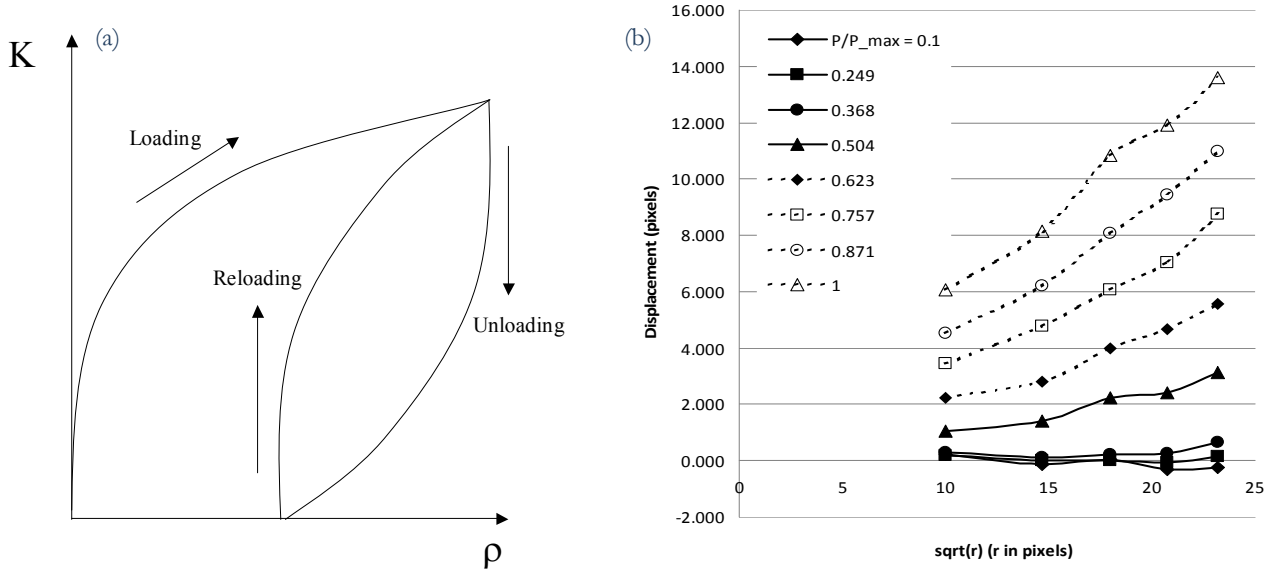


Figure 5: (a) Schematic of crack behaviour in K / ρ space (after Pommier et al [20]); (b) Analysis of crack displacements according to the elastic-plastic model (Eq. (4)) – loading part of the cycle.

The experimental results described above can be used to investigate the validity of this approach. Within the framework of the model, the relative displacement of the crack faces will be a superposition of that caused by the elastic and plastic parts of the field. Namely

$$u_y(r) = \frac{8K_I}{E} \sqrt{\frac{r}{2\pi}} + \rho \quad (4)$$

Hence, a plot of u_y against \sqrt{r} should give a straight line with a gradient of $8K_I/(E\sqrt{2\pi})$ and an intercept of ρ . Fig. 5(b) shows the same data as in Fig. 4(a) interpreted in this way. It can be seen that the displacement data do, indeed, give straight lines when plotted in this manner, but that the intercepts (corresponding to ρ) are relatively small. This is unsurprising, given the good fit of the elastic model (Fig. 4). We should also note that for the loading phase, values of ρ obtained are generally negative, which does not make physical sense. However, positive values are obtained if the data for the unloading part of the cycle are analysed and there is therefore some evidence of the hysteresis type of behaviour shown in Fig. 5(a), even though the values of ρ are incorrect and the shape of the loop is also not as expected. In interpreting this data, we should recognise that, as noted above, the crack tip position can be difficult to estimate in the DIC images. We therefore re-analysed the data using a range of possible crack tip offsets to adjust the position of the crack tip relative to the first measurement. Figure 6a shows the results of such a calculation with a crack tip offset of -60 pixels (i.e. with the crack tip positioned 40 pixels or $37.2 \mu\text{m}$ from measurement point 1 (Fig. 2)). It can be seen that the data still produces reasonable straight line variations of displacement with \sqrt{r} . The correlation coefficients obtained for $P/P_{max} > 0.5$ lie in the range $0.939 < R^2 < 0.987$, compared to $0.954 < R^2 < 0.993$ for the case with no offset. A similar plot can be obtained for the unloading part of the cycle, and the variation of K and ρ can be plotted for a complete cycle, to produce an experimental graph in the same form as Fig. 5a. The resulting plot is shown in Fig. 6b.

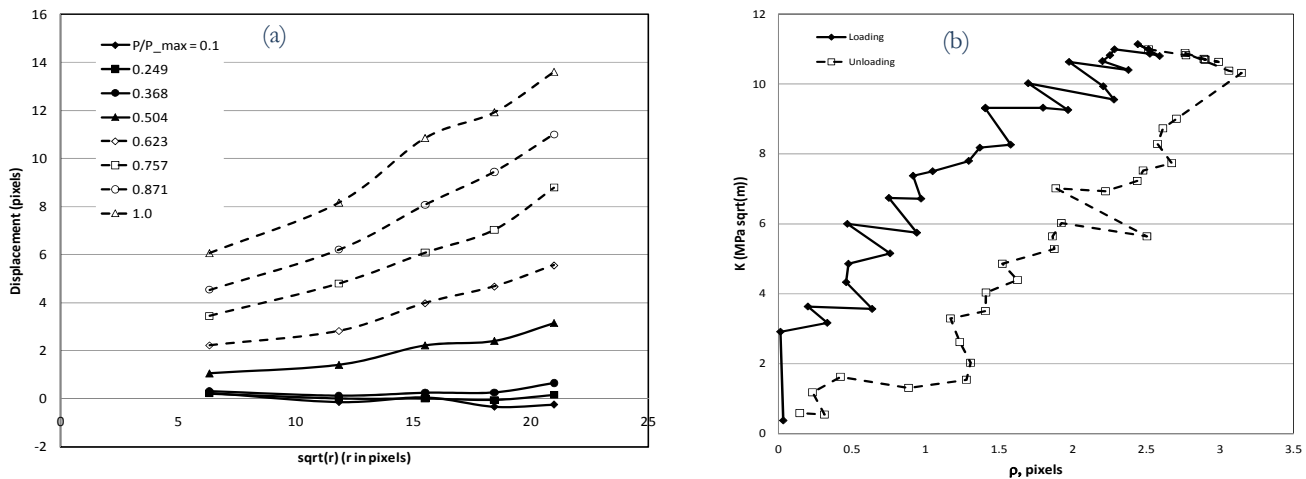


Figure 6: (a) Analysis of crack displacements according to the elastic-plastic model (Eq. (4)) – loading part of the cycle. Crack tip offset = - 60 pixels (- 55.8 μm); (b) variation of K and ρ for a complete cycle, Crack tip offset = - 60 pixels.

The opportunity has been taken in Fig. 6b to plot data corresponding to all of the loads captured in the experiment where the crack is open ($P/P_{max} > 0.35$). This gives some measure of the amount of scatter experienced. It will be seen that the results exhibit qualitatively the hysteresis behaviour predicted by Pommier's model (Fig. 5a and [20]). There are, however some differences. In particular, it appears that the measured value of ρ continues to increase slightly for a short while after the load is reversed, although as expected the measured value of K starts to fall. This does not seem to be physically sensible. Some preliminary investigations show that this 'overshoot' can be eliminated by increasing the negative offset to about -90 pixels, although such a value would suggest that the crack tip is very close to the first measurement point, which is not what was thought to be the case when the original experimental results were recorded.

DISCUSSION AND CONCLUSIONS

The paper has described a set of digital image correlation measurements made on propagating fatigue cracks in 6082 T6 aluminium. These were originally made with the objective of examining fatigue crack closure on three different thicknesses of CT specimen. In the current paper, some of the original results have been re-analysed to give the variation of crack profile against load for a complete loading cycle. The results appear to fit reasonably well to the classical elastic model of near tip displacements and quantitative information can be obtained for the corresponding stress intensity factor. The results show that the variation of K with load is relatively close to that expected from the stress intensity factor solution for the specimen geometry, but that there is a significant negative residual K caused by the contact stresses during the crack closure phase of loading.

The same data has also been analysed according to the elastic-plastic model proposed by Pommier and co-workers [20]. The results show that small negative values of crack tip opening, ρ , are obtained when the nominal position for the crack tip is assumed. If the crack tip position is adjusted, more physically-representative values can be obtained and there is some evidence of the hysteresis behaviour predicted by Pommier's model. This hysteresis behaviour contrasts with that observed using the elastic model, where the relationship between load and stress intensity factor is virtually the same during loading and unloading. The dependence of the results on the assumed position of the crack tip is not unexpected, but there appears to be a relatively wide range of positions which produce acceptable results. A robust means of identifying the 'best fit' position is therefore required.

Space considerations preclude a comprehensive presentation of the results here, and we have concentrated on analysing the data obtained from a single specimen at a single crack length. The data originally collected by de Matos [21] is far more comprehensive than that presented here, consisting of measurements from 20 specimens at three different thicknesses and, typically, around 25 crack lengths per specimen. The majority of this data remains to be analysed. It should also be pointed out that the results presented here have only analysed the displacements at the five locations



chosen by de Matos for the DIC calculations. Should more data be required, it would be possible to re-analyse the original videos to give displacement information at a wider range of locations.

The work presented demonstrates the power of the digital image correlation technique for work of this nature and suggests that further experimental work of this nature has much to offer in furthering our understanding of crack tip stress fields in propagating fatigue cracks.

ACKNOWLEDGEMENT

P.F.P. de Matos would like to gratefully acknowledge the support of the Portuguese Fundação para a Ciência e a Tecnologia (FCT) for providing a D.Phil. scholarship (reference SFRH/BD/12989/2003, financed by POSI).

REFERENCES

- [1] R.J. Sanford, Selected Papers on Foundations of Linear Elastic Fracture Mechanics, SEM/SPIE, USA (1997).
- [2] R.J. Sanford, Selected Papers on Crack Tip Stress Fields, SEM/SPIE, USA (1997).
- [3] C.E. Inglis, Trans of the Institution of Naval Architects, 55 (1913) 219.
- [4] H.M. Westergaard, Jnl Appl. Mech., 6 (1939) 49.
- [5] G.R. Irwin, Jnl Appl. Mech., 24 (1957) 361.
- [6] A.A. Griffith, In: Proc. 1st Int. Conf. for Appl. Mech., Edited by Biezeno and J.M. Burgers, (1925) 55.
- [7] P. Paris, F. Erdogan, Jnl of Basic Eng, 85 (1963) 528.
- [8] J.R. Rice, Jnl Appl. Mech., 35 (1968) 379.
- [9] O.C. Zienkiewicz, R.L. Taylor, The Finite Element Method, Butterworth-Heinemann, UK (2000).
- [10] P.F.P. de Matos, D. Nowell, Eng Fract. Mech., 75 (2008) 2087.
- [11] P.F.P. de Matos, D. Nowell, Int. Jnl Fatigue, 30 (2008) 1930.
- [12] A.A. Wells, D. Post, S.E.S.A. Proceedings, 16 (1958) 69.
- [13] A.J. Rosakis, Eng. Fract. Mech., 13 (1980) 331.
- [14] P.B. Crosley, S. Mostovoy, E.J. Ripling, Eng. Fract. Mech., 3 (1971) 421.
- [15] M.A. Sutton, W. Zhao, S.R. McNeill, J.D. Helm, R.S. Piascik, W.T. Riddell WT, ASTM Special Technical Publication, 1343, (1999) 145.
- [16] P. Lopez-Crespo, D. Camas-Peña, A. Gonzalez-Herrera, J.R. Yates, E.A. Patterson, J. Zapatero, Key Engineering Materials, 385-387(2008) 369. Journal of Fatigue, 31, 11-12, 1795.
- [17] S.R. McNeill, W.H. Peters, M.A. Sutton, Eng. Fract. Mech., 28 (1987) 101.
- [18] N. Limodin, J. Rethore, J.Y. Buffiere, Acta Materiala, 58 (2010) 2957.
- [19] P.F.P. de Matos, D. Nowell, Int. Jnl Fatigue, 31 (2009) 1795.
- [20] D. Nowell, P.F.P. de Matos, Procedia Engineering, 2 (2010) 1035.
- [21] S. Pommier, R. Hamam, Fatigue Fract. Engng. Mater. Struct., 30 (2006) 582.
- [22] P.F.P. de Matos, D.Phil. Thesis, University of Oxford, UK (2008).
- [23] Questar QM1 long-distance microscope, Questar Corporation, New Hope, PA, USA.
- [24] C. Eberl, R. Thompson, R. Gianola, Digital Image Correlation and tracking with Matlab, Matlab Central file exchange (2006).
- [25] M.F. Kanninen, C.H. Popelar, Advanced Fracture Mechanics, Clarendon Press, UK (1985).
- [26] H.L. Ewalds, R.J.H. Wanhill, Fracture Mechanics, Edward Arnold, UK (1984).